Arab J Geosci (2011) 4:785–801
DOI 10.1007/s12517-009-0090-9

ORIGINAL PAPER

Runoff modeling of the wadi systems for estimating flash flood and groundwater recharge potential in Southern Sinai, Egypt

Alaa A. Masoud

Received: 31 March 2009 / Accepted: 3 September 2009 / Published online: 25 September 2009

Abstract Evaluating the likelihood of a flash flood as well as flood water resource is vital for establishing properly sustainable developments in arid environments. However, the high degree of spatial and temporal variability in hydrometeorological processes and the general lack of suitable data limit these efforts. In the present work, a runoff model, adopting the simple Soil Conservation Service method, was built for 13 ungauged catchments in Southern Sinai, Egypt. Runoff modeling was conducted as a function of the descriptive parameters of the catchments, and the maximum average rainfall occurred in 1 day in the period 1960–1990, designed according to a storm event recorded at the outlet of one of the studied catchments on the 2nd of November 1994. The catchments' descriptive parameters were extracted from available remote sensing data and field investigations. Land covers including road networks and 83 rock-soil types were also extracted from the maximum likelihood classification of the Landsat-7 ETM+ imagery. The catchments were then subdivided into 103 smaller subcatchments, which were then placed into different terrain types according to hydrologically relevant surface characteristics. Hydrologic characteristics and soil type(s) in the subcatchments were estimated during on-site visits. Morphometric parameters of the wadi catchments and the channel networks were derived from the analysis of the SRTM3 digital elevation model (DEM). Hydrographs were drawn and routed to the main catchment outlets based on appropriate wadi dimensions and roughness using the Muskingum's method. The runoff and infiltration volumes were quantified. The resulting models have been used to investigate the relative potential for flooding and the groundwater recharge in the catchments. Further, in order to determine specific sites with a high potential for flood risk and groundwater recharge, decision-ruled integrated analysis of the generated GIS layers describing relative stream power and wetness indices were applied. Due to the lack of flow data, the results of the hydrological models were validated against the DEM-derived relative stream power and the wetness indices as well as against field checks and available reports as an alternative. The results of this study could help to prioritize areas where flood control measures should be directed, as well as effectively augment management plans for the appropriate development of water resources.

Keywords SCS runoff modeling · Relative stream power · Wadi systems · Southern Sinai Peninsula · Egypt

A. A. Masoud (✉)
Geology Department, Faculty of Science, Tanta University,
Tanta 31527, Egypt
e-mail: alaamasoud@hotmail.com

Introduction

In arid regions the world over, flash floods are a major cause of loss in infrastructure, property, and human life. Despite this, under ideal circumstances, flood water could be used to constitute a considerable amount of a region's water resources, and also be utilized to fulfill part of the increasing water demand in areas prone to flooding that are currently experiencing high population growth and economic development. This is especially true in the case of the wadi systems in the Southern Sinai Peninsula of Egypt, where flash floods have become an unfortunate annual occurrence. Due to the difficulties in acquiring runoff data and the extensive spatial and temporal variability of the rainfall, there is a general lack of hydrometeorological data that makes runoff less predictable and rainfall–runoff

processes more difficult to analyze. In addition to the harsh climate, the wadi reaches are located far away from settlements, becoming muddy and inaccessible after flooding due to the absence of vegetation. Also, flood water carries a large amount of sediments, which typically damage measuring devices. However, this water is essential to communities and sustains tourism-based enterprises in the area. Despite this, very little attention has been directed at understanding the dynamics of the runoff process characteristic of such wadi systems. In the absence of flow data, runoff modeling could be a promising approach to enhance the livability of the area and any surrounding landscape with similar physiographic conditions (Foody et al. 2004; Gheith and Sultan 2002).

For the purpose of predicting hydrologic responses in ungauged catchments in arid areas, the Soil Conservation Service curve number models (SCS 1972) are widely used. These models require a reduced number of terrain parameters that are extractable from Geographic Information System (GIS) layers, which can then be verified during on-site visits. Such models rely greatly on expert knowledge to relate observable physical catchment descriptions to the dynamic hydrologic response during a storm event (Sefton and Howarth 1998; Littlewood 2002; Kokkonen et al. 2003). SCS models are considered to serve as well as, or even better than, more complex models in terms of predicting rainfall–runoff in gauged and ungauged catchments (e.g., Michaud and Sorooshian 1994; Wagener et al. 2004). In the US, SCS models were widely applied on many ephemeral catchments (Hickok et al. 1959; Gray 1961; Headman 1970). Murphey et al. (1977) draw relationships between hydrograph time to peak, duration, mean peak discharge, volume, peak–volume ratio, and basin parameters such as area, shape, slope, drainage density, and basin relief, as well as a combination of these parameters. The structure of the hydrologic response is found to be intimately linked to the geomorphologic parameters of the catchment (Valdes et al. 1979; Sharma and Murthy 1995). The input parameters and the models of the ungauged catchments are commonly derived from extrapolation of (or interpolation between) verified data and models of the nearby gauged catchments, where the degree of hydrological similarity between catchments dictates the degree of similarity between their input data and the built models. Model calibration and validation is another difficult and a crucial issue, and these should be tailored to the objectives of the study and for the types of applications for which it is intended (Schlesinger et al. 1979; Klemeš 1986; Beven 1996; Refsgaard 1997; Duan et al. 2003; Ajami et al. 2004; Moussa et al. 2007). In the Eastern Desert of Egypt, the synthetic SCS runoff model was successfully applied on unguaged catchments for estimating wadi runoff and groundwater recharge (Gheith and Sultan 2002), as well as for predicting locations sensitive to flash flooding (Foody et al. 2004). Gheith and Sultan (2002) extrapolated the spatially distributed precipitation with respect to topographic elevation from weather stations located on the Nile Valley and the coast of the Gulf of Suez and the Red Sea. Due to the absence of real discharge data, Gheith and Sultan (2002) based their model validation on field observations. Foody et al. (2004) assumed a rainfall event of 30 mm/h with a duration of 2 h to build their models and used the road damage observations to validate their models.

In the present research, hydrologic responses of the 13 largest ungauged catchments in the Southern Sinai Peninsula were predicted using the SCS models. The prime objective is to highlight the maximum possible flash flood and groundwater recharge potentials of the catchments, as well as demarcate flood risk-prone sections of road networks and sites with possibly high groundwater recharge potential integrating several GIS layers. Since the aim is to assess the relative potential of the catchments to flood risks and groundwater recharge and since model parameters were derived either directly from field data or indirectly through experiences from values in similar catchments, the interpreted results of the final models were only validated against topographic indices derived from the DEM as well as against field observations and the available flash flood reports as an alternative.

Study area

The study area spans across 21,400 km^2 of the Southern Sinai Peninsula (Fig. 1). Its climate, physiography, geomorphology, and lithostructural characteristics are strongly interrelated and have a great bearing on the catchment drainage and groundwater potential. The landscape is a natural desert with scant natural vegetation located in the Mediterranean arid zone. The coldest month is December with occasional freezing (low temperatures of −4°C) in January at the summit of Saint Catherine Mountain (2,641 m asl). The period between June and August is the warmest of the year, with temperatures as high as 45°C. The temperature is affected by the altitude and proximity to the sea. Rainfall is highly irregular (both in time and space) and rain storms are more likely to occur as infrequent (e.g., every other year) large events or as rare (every 5–60 years) extreme events. The terrain is characterized by a high variability of relief, with ridges and mountain ranges adjacent to lowlands, a significant factor in the generation of overland flow. The lack of vegetation cover over the wadi beds results in no protection from raindrop impact, so the overland flow, concentrated by the topography, either converges downstream in a complex network of deeply cut

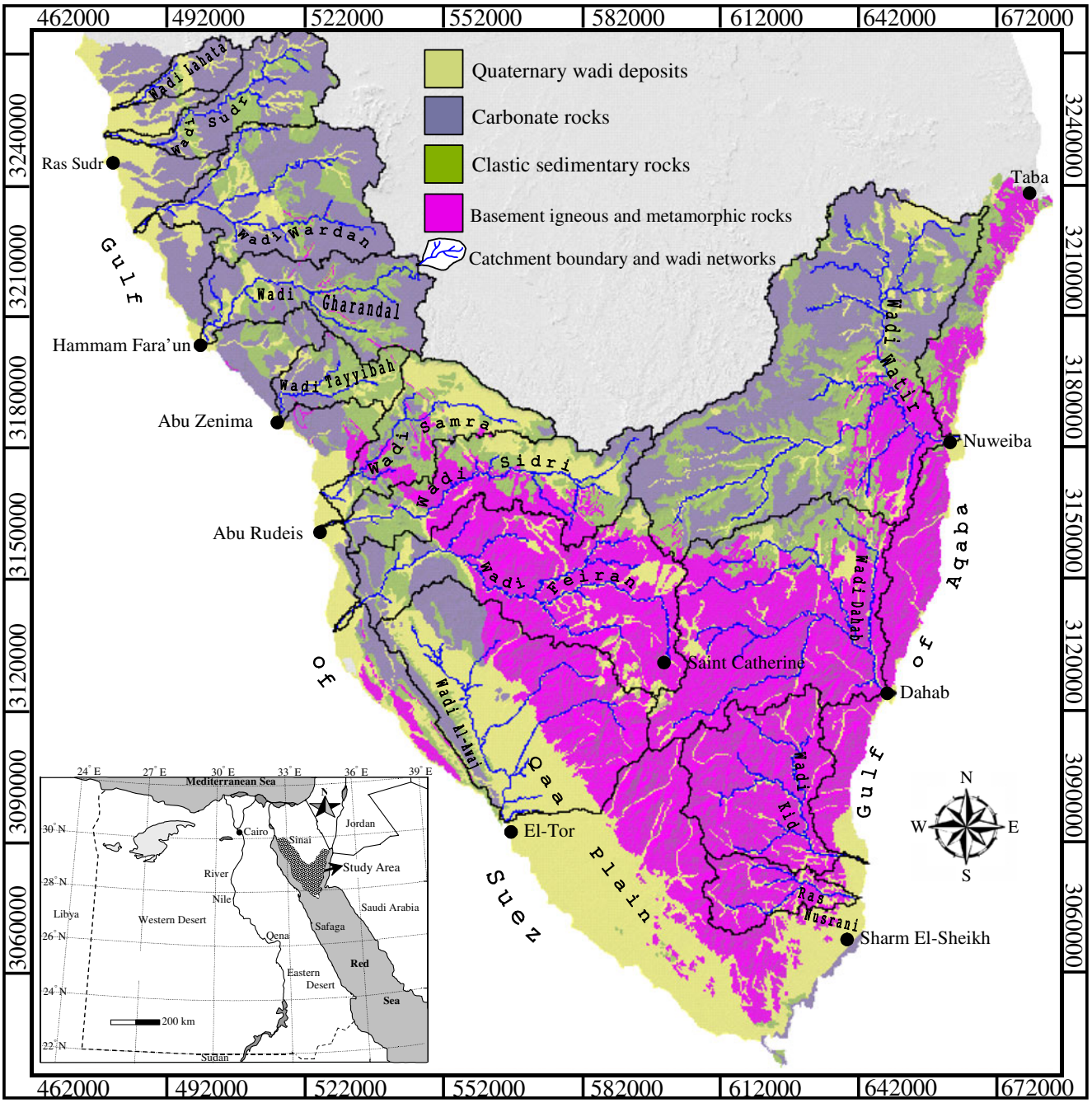

Fig. 1 Location and physiographic features of the study area

wadis to the Gulfs of Aqaba and Suez, or permeates the soil and recharges the subsurface aquifers. Flash floods in this area often produce much erosion and sedimentation that cause damaging effects on the road networks and structures in local major cities, which are built on the outlets of the major hydrographic catchments. These floods often hamper supporting several cities (e.g., Nuwibie, Dahab, Sharm El-Sheikh) and many coastal resorts with drinking water and food, resulting in a multitude of environmental and economic consequences, in addition to the loss of life and property.

Geologically, the area is an uplifted horst bordered by the graben system of the Gulfs of Aqaba and Suez, and is a part of the Precambrian Arabian-Nubian Massif that extends across southern Sinai, the Eastern Desert of Egypt, Sudan, and western Saudi Arabia. Different rock units with distinct hydrogeological properties range from the Precambrian basement (34.36% coverage) to the Phanerozoic sedimentary succession (Fig. 2). The sedimentary succession includes a wide range of geologic ages. It is divided by Said (1962) into three divisions: (1) the lower clastic

Fig. 2 Photograph showing wadi floor deposits, Carboniferous sandstones (*front*), and the basement rocks caped by Paleozoic sandstone (*back*)

division, which overlies the Precambrian igneous and metamorphic rocks and extends to the Lower Cretaceous Nubian Sandstone (15.79% coverage); (2) the middle calcareous division, which ranges in age from Cenomanian to Eocene and covers about 24.32% (fractured limestone, chalky limestone, chalk, shale, marl, and dolomite); and (3) the upper clastic division of the Neogene to Holocene age composes about 25.52% of the area and is distributed in the wadi floors, catchment outlets, and sedimentary plains including the Sudr and Qaa Plains. Groundwater exists in a variety of water-bearing formations, including fractured crystalline basement rock, Nubian sandstone, fractured and karstified Carbonate, and in several types of younger deposits, such as alluvial deposits and eolian sand (Dames and Moore 1985).

The catchments involved in this study were named according to the main wadi flowing from the catchment divide downstream to the outlet, except for the catchment of Ras Nusrani, which was named after a granite mountain in the region.

Materials and methods

Because runoff modeling is meant to be used on ungauged catchments, the only data available for modeling were those of the precipitation, topography, landcover information, and wadi hydrogeometric/roughness characteristics that were measured from the thematic data and verified during on-site visits. Precipitation information was derived from scanned isohyet map showing the spatial distribution of the average maximum daily rainfall. The SRTM3 DEM of the 3-arc second grid spacing (90 m) was used to represent the topography. Land cover data composed mostly of the bedrock lithology and soil cover were extracted from four Landsat-7 ETM+ with world reference system (WRS) information and acquisition dates, as shown on Table 1. The available geological maps (scale 1:250,000, sheets No. 1, 2, and 3) of the Geological Map of Sinai (1994) were scanned at 254 dpi and utilized in training/verification classes derived from the image data. The GRASS GIS package (GRASS Development Team 2006) was used for the integrated analysis of the produced catchment GIS layers. Field investigations were carried out to validate and update the derived GIS layers used to build the hydrographs. A windows-based software was developed using Visual Basic to automate the process for calculating excess runoff and the unit hydrograph (UH), convolute the UH for the whole catchment, and route the flow of flood waves to the catchment outlet. The software is available for free at the author's website (http://alaamasoud.tripod.com). For the sake of visual clarity, intermediate results are shown for the catchment of Wadi Watir with final results shown for the whole studied catchments. The methodology adopted is represented by a flow chart shown on Fig. 3 and described in detail in the following sections.

Table 1 Landsat-7 ETM+ images used for lithologic classification

WRS-2 path/row	Date, year-month-day
174/040	2000-09-10
174/041	2000-09-10
175/039	2000-12-22
175/040	2000-12-22

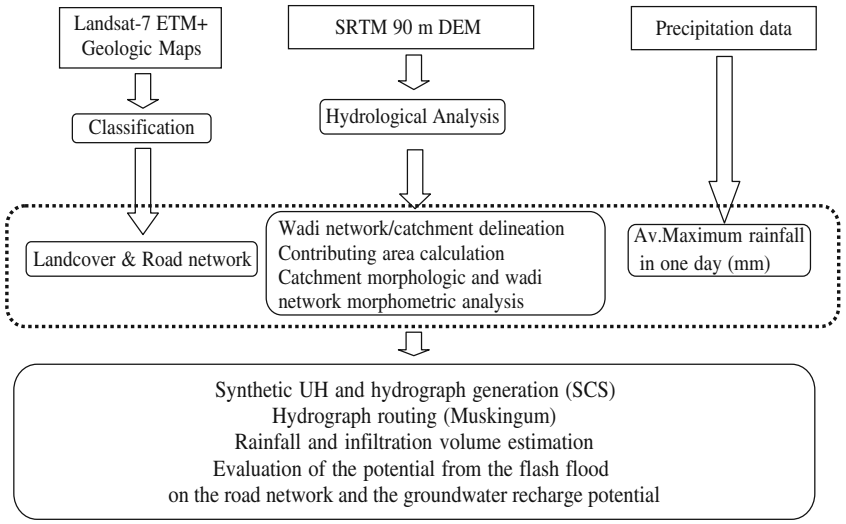

Fig. 3 Flow chart of the adopted methodology

Hydrological analysis of DEM

The Shuttle Radar Topography Mission (SRTM) 90 m DEM data (Farr and Kobrick 2000) was available for the area. Seven 1-degree coverage DEM tiles were patched together and processed prior to all subsequent analysis. Flat areas and depressions like pits and sinks in DEM interrupt flow paths and alter drainage directions. These problematic areas were modified in a way to permit continuous flow from the ridges down to the outlets using Jenson and Domingue's (1988) algorithm for enforcing flow on flat areas, and the impact reduction approach (IRA) of Lindsay and Creed (2005) was used to circumvent the depressions in DEM.

The shape of the catchments and their channels determine how water is transmitted through the catchment. Catchment area, length, shape, elongation, and relief, as well as channel length, frequency, and bifurcation influence the amount of water yielded, affecting the rate of water discharge. Flow routing algorithms are commonly used to derive such various terrain attributes. Many flow routing algorithms are available, including D8, FD8 (Freeman 1991; Quinn et al. 1991), D-infinity (Tarboton 1997), and the Quinn et al. (1995) modification of FD8. These algorithms differ in how to model flow direction and divergence, and thus handle stream networks and the specific catchment area differently. In this study, each technique was applied and tested. The simplest D8 method performed satisfactorily and was used accordingly. Delineation of the subcatchments and the wadi networks, as well as their geomorphologic and morphometric characteristics were carried out using hydrologic modules in the GRASS GIS package (GRASS Development Team 2006). Wadi Watir has 32 of the 103 delineated subcatchments from the whole study area, with sizes ranging from 2 to 372 km^2. Delineated subcatchments for Wadi Watir with their channel networks are shown on Fig. 4. Geomorphologic/morphometric characteristics of the main catchments and their channel networks are shown on Table 2. These characteristics included the catchment area, length (L), length from the catchment oulet to its centroid (L_c), divide average relief, maximum wetness index (WI), main channel length, total channel length, main channel slope in percentage, and stream orders.

Landcovers and soil hydraulic properties

Landcover classes were derived from a supervised maximum likelihood classification of the Landsat-7 ETM+ data, using training classes derived from the geological maps. Reasonable results were obtained from the classification method where the kappa coefficients of Congalton (1991) showed an average commission of 90% for the 83 types of rock and soil identified throughout the whole area. Outcroppings of different rock-soil types at Wadi Watir are shown on Fig. 5. To define different hydrological groups predominant on the subcatchments, measurements of steady-state infiltration rates were carried out in several test sites in the wadi floor along the water courses. This was performed through in-situ rainfall simulation at a 1 m^2 scale under 40 mm h^{-1} rainfall intensity for 1 h. The observed capacities ranged from 6.7 to 12.9 cm h^{-1} in all test sites. Similar values have been reported in the eastern desert of Egypt in Foody et al. (2004).

Derivation of precipitation

In the present research, the only available precipitation records for the area were in the form of isohyet maps describing the average maximum rainfall (millimeter) recorded in 1 day. These data were generated from the historical precipitation archives (1960–1990) by the Egyp-

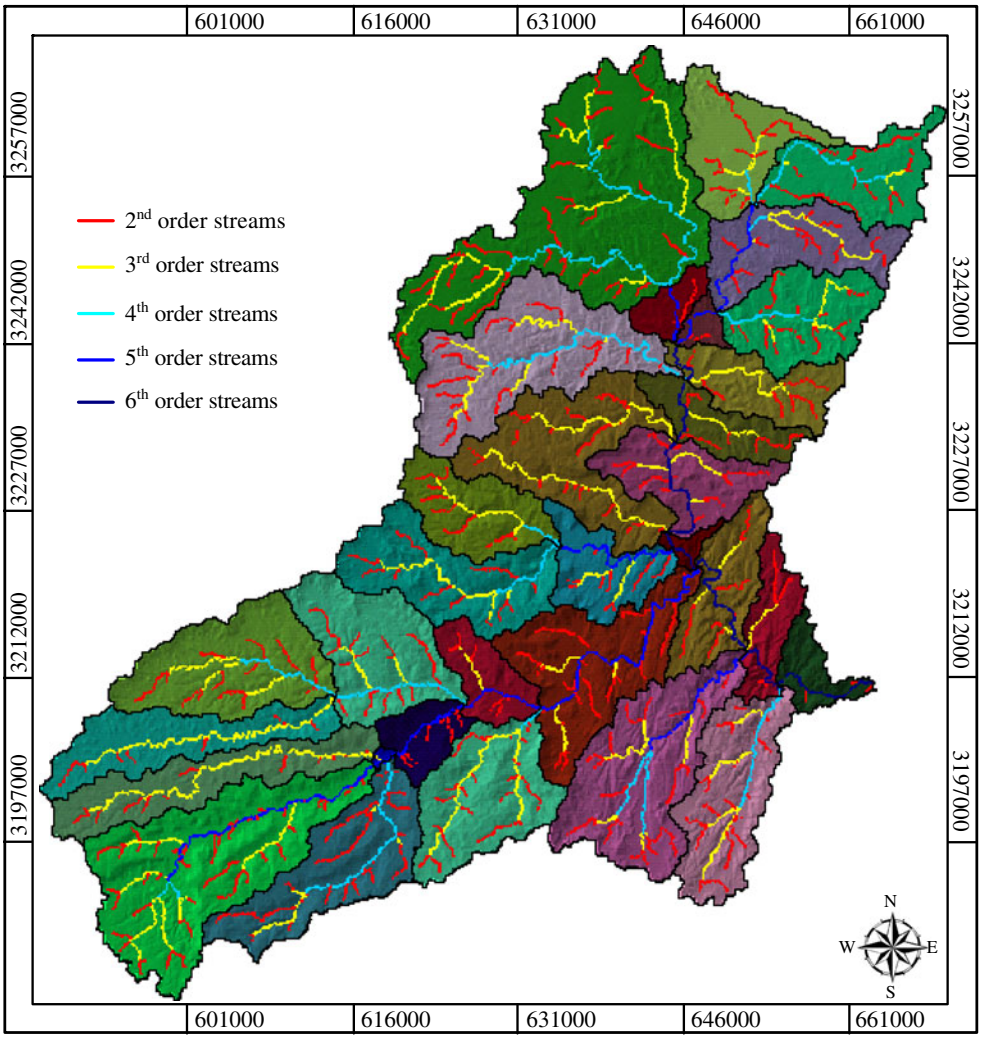

Fig. 4 W. Watir subcatchment boundaries with wadi network strahler orders draped over DEM. First order streams are not shown for the sake of visual clarity

tian Meteorological Authority in 1996. These maps were digitized and converted into a GIS layer; the inter-isohyet area was interpolated using an algorithm that approximates the surface iteratively through potential mechanical energy minimization until a rendering of the final surface could be produced using the least mean-squared error optimization technique. More details on the surfaces generated with this technique are described in Masoud (2003). Rainfall records for 2 November 1994 were only available for the El-Tor station, which is located 2 m above the mean sea level at the outlet of the Wadi Al-Awaj catchment. However, such records do not represent the actual rainfall throughout the basin due to orographic effects where strong precipitation gradients are accentuated with elevation of the nearby mountain ranges. To overcome this problem, and to predict the amount of rainfall over the whole catchment, a pixel-based correlation analysis was performed comparing elevation data of the DEM and the average maximum rainfall (millimeter) in 1 day. A correlation coefficient of 0.9 was achieved. This method was then applied to the ungauged catchments and rainfall amounts were estimated for the subcatchments. The estimated rainfall amounts for the subcatchments were then designed based on the 2 November 1994 storm. The precipitation over the catchment of W. Al-Awaj where El-Tor station is located on its outlet was estimated at 51.3 mm that is in accordance with the value of 60 mm reported in Gheith and Sultan 2002, on the Red Sea mountains proximal to El-Tor station during the 1994 storm event. Thus, the precipitation estimates over the studied catchments are reasonable.

Developing the soil conservation service model

The Soil Conservation Service (SCS 1972) method was originally designed for small humid agricultural catchments in the USA, and has since been adapted to measure infiltration losses in arid areas of Saudi Arabia and the USA (Graf 1988; Walters 1990) with similar climatic and physiographic conditions. This method can be applied equally well to larger catchments, taking into account the

Table 2 Characteristics of the main catchments and their channel networks

Catchment	Area (km^2)	L (km)	L_c (km)	Divide average relief (m)	Max. wetness index	Main channel length (km)	Total channel length (km)	Total channel no.	Main channel slope (%)	Stream orders
W. Watir	3,459	76	28.5	1036	29.2	110.5	5,070	2,450	5.05	6
W. Dahab	2,069	57	37.4	1,272	28.9	99.1	2,951	1,386	9.53	6
W. Kid	1,038	50	38.5	1,119	28.3	74.0	1,265	605	7.42	6
Ras Nusrani	365	36	23.4	773	27.2	53.7	546	272	5.41	5
W. Al-Awaj	1,950	57	22.5	922	28.6	83.0	1,250	1,290	1.46	7
W. Feiran	1,783	81	52.2	1,059	28.8	143.2	2,702	1,307	3.79	6
W. Sidri	1,062	79	39.2	885	28.2	106.7	1,622	769	4.12	5
W. Samra	714	55	35.1	504	27.9	80.4	1,184	551	4.56	5
W. Tayyibah	358	33	19.8	530	27.2	54.5	518	252	3.42	5
W.Gharandal	862	54	36.5	625	28.0	91.2	1,400	697	3.2	5
W. Wardan	119	59	29.6	508	28.4	85.3	2,048	1,002	3.66	6
W. Sudr	595	54	34.3	424	27.7	81.5	1,022	475	3.07	6
W. Lahata	190	32	16.0	341	26.3	44.4	292	120	5.01	5

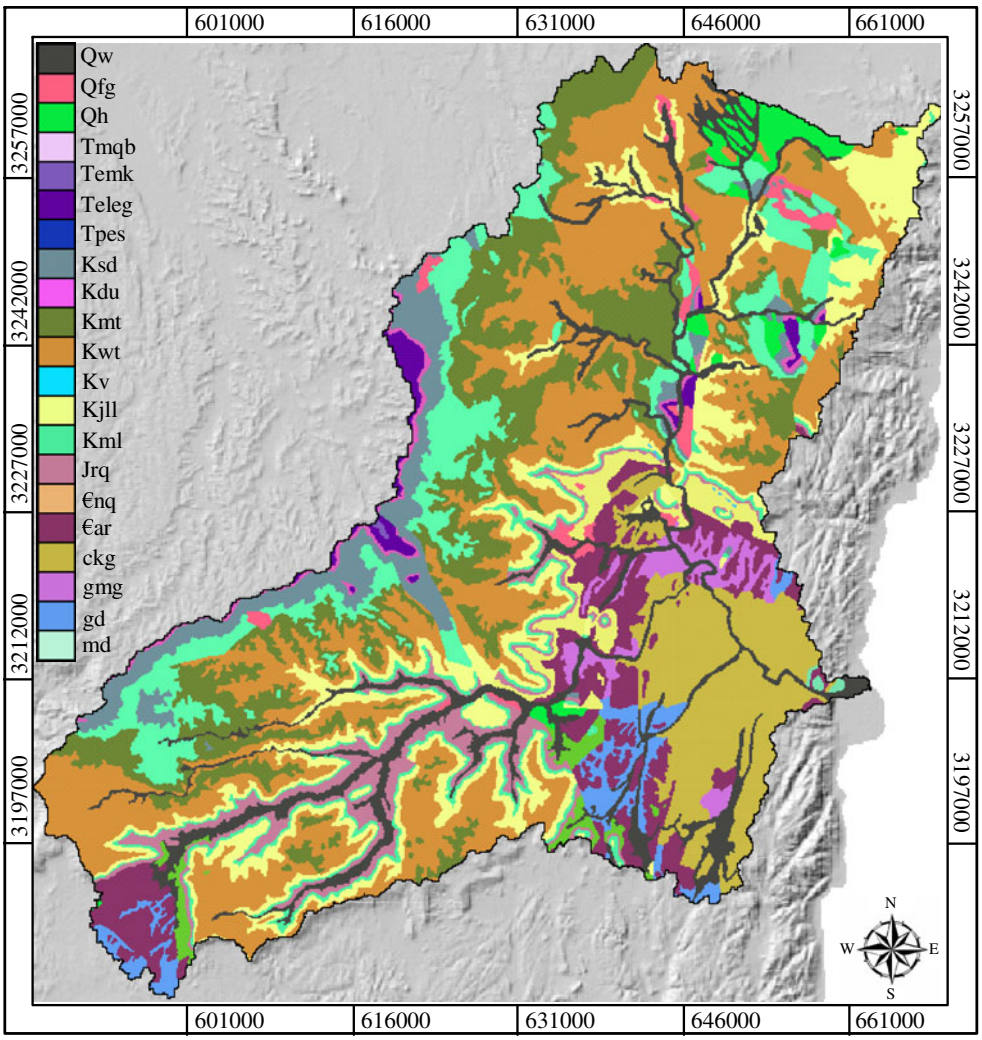

Fig. 5 Different rock-soil types of W. Watir catchment with codes shown on Table 3

geographical variations of rainfall from storms, as well as rock-soil-cover complexes, by working with small hydrologic units of the catchments. Runoff modeling in arid environments counts for the separation of the Hortonian overland flow (runoff or infiltration excess) and the infiltration losses in the dry wadis. Runoff occurs when the storm intensity exceeds the infiltration capacity of the wadi soil (e.g., Yair and Lavee 1985; El-Hames and Richards 1994). Primarily based on empirical equations, unit hydrographs can be synthesized for ungauged catchments by relating the unit hydrograph's shape to catchment characteristics such as basin length and area (Yen and Lee 1997). The SCS runoff curve number method is used to abstract the total rainfall hyetograph into the effective rainfall hyetograph, and to model the hydrographs at each subcatchment outlet, relating hydrograph characteristics (lag time, peak discharge, base time, etc.) to catchment parameters (area, length, hydrologic characteristics, soil cover types, etc).

Given the hyperarid conditions, paucity of vegetation, and rugged topography of the region, only abstractions due to infiltration are considered. The SCS method estimates precipitation excess as a function of the cumulative precipitation, rock-soil cover, land use, and antecedent moisture, using the following equation:

$$Q = \frac{(P - 0.2S)^2}{(P + 0.8\,S)} \text{ and } F = P - Q \tag{1}$$

where F is the total infiltration depth (millimeter) and S represents the soil retention parameter (millimeter). For each time step, the overall sum of rainfall P was calculated, and Q and F curves were deduced for each subcatchment. These curves are standardized through the dimensionless curve number CN, which is defined between 30 and 100. S is estimated as:

$$S = 254\left(\frac{100}{\mathrm{CN}} - 1\right) \tag{2}$$

The initial abstraction is related to S according to different regions, and is commonly defined as 0.2 S in arid catchments. CN is a hydrologic rock-soil-cover coefficient showing the runoff potential on the catchment as represented by a combination of hydrologic soil groups and the soil Antecedent Moisture Condition (AMC) for the 5 days preceding a given storm event. The Antecedent Moisture Condition I (AMC-I) with the lowest runoff potential was proposed for the studied catchments, taking into consideration that both rainfall is rare throughout the year and soil would have been dry before any storm event. Various rock and soil types were assigned an appropriate CN based on their physical and hydrological characteristics as verified in the field. These types fall into four main general groups: hard rock cover comprised of igneous and metamorphic bedrock, clastic sandstones, calcareous carbonate rocks, and the Quaternary alluvial deposits as shown in Fig. 1. Different hydrologic groups in the subcatchment are tabulated as a percentage of the total subcatchment area with its corresponding CN. A weighted average CN is then generated. As a first step, the SCS method was applied to separate precipitation from the excess runoff and initial loss. The achieved results are shown for W. Watir in Fig. 6. The excess runoff was then used to draw the UH for the subcatchments.

The most significant parameters that shape the UH are the peak discharge (q_u) and lag time (T_{lag}). The UH peak discharge q_u resulting from incremental excess precipitation of 1 mm occurring over the drainage area in a specified time is a function of the lag time (T_{lag}), drainage area, and a peak factor C given by the equation:

$$q_u = \frac{C\ A}{T_{lag}} \tag{3}$$

where q_u is the unit peak discharge ($m^3/s/km^2/mm$) of runoff; A is the catchment area in km^2; C is the peak rate factor (that has been known to vary from about 0.258 in steep terrain to 0.129 in very flat areas); and T_{lag} is the lag time to peak runoff (hours), estimated as the time difference between the center of mass of the effective rainfall hyetograph and the center of mass of the direct runoff hydrograph. The lag time is related to the catchment length, average slope, and Manning roughness coefficient (n) as follows:

$$T_{lag} = 24n\left(\frac{LL_{ca}}{\sqrt{S}}\right)^{0.38} \tag{4}$$

where L is the length of the longest water course in miles; L_{ca} is the length along the longest water course to the subbasin

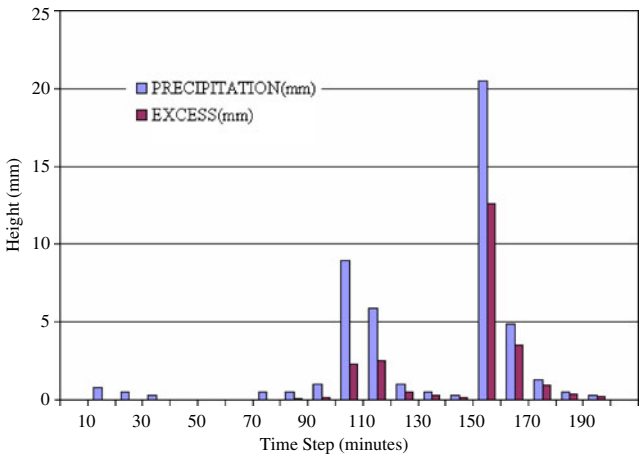

Fig. 6 Rainfall and excess runoff depths for W. Watir

centroid in miles; and S is the overall slope of the longest water course in feet per mile. The Manning coefficient, n, is the average value estimated for the wadi networks in the subcatchments. "Roughness values" set at 0.05 for mountainous areas, 0.03 for foothills, and 0.015 for valleys have been adopted here for the landform classes extracted from the DEM based on slope classification. The UH was drawn for a time interval of 10 min convoluted to calculate a flood hydrograph at each subcatchment outlet for the storm duration (Chow et al. 1988). Peak discharge of the catchment hydrograph, q_p was then computed using Eq. 5 below:

$$q_p = q_u A \; Q \tag{5}$$

where Q is the depth of the direct runoff in millimeters.

Hydrographs corresponding to each subcatchment were combined and propagated according to Muskingum's method (Cunge 1969). This flow routing method has a wave celerity parameter K (meters per second) along the subcatchment that reaches downstream, as well as a dimensionless parameter X ranging from 0 to 1 describing the relative importance of the effects of inflow rates on defining the amount of stored water in the reach. Estimates for the wadi dimensions, such as hydraulic radius and the wadi slope, were extracted from the DEM and verified during a site visit. Appropriate values of K and X were selected for different wadi reaches in each subcatchment. The final flood outflows at each catchment outlet were then quantified. As the catchments are all ungauged, and also due to the absence of flow records, no model parameter calibration test was performed since all parameters were derived either directly from field data or indirectly through experiences from values in similar catchments.

Groundwater recharge and flash flood potentials

Groundwater recharge from infiltration losses

Estimating transmission losses in arid environments is difficult because of the variability of surficial geomorphic characteristics and infiltration capacities of soils and near-surface low-permeability geologic layers (e.g., calcrete). Losses occur as flow infiltrates channel bed, banks, and floodplains. Transmission losses in ephemeral channels are nonlinear functions of discharge and time (Lane 1972), and vary spatially along the channel reach and with soil antecedent moisture conditions (Sharma and Murthy 1994). Without the proper management of this water resource, the excess precipitation can be quickly lost to the high evaporative environment or lost from the watershed via runoff.

In general, as soil on the wadis is dry preceding winter storms with negligible evaporation, the alluvium underlying the wadi beds are assumed to effectively transmit infiltration losses down to the subsurface alluvial aquifers. Wadi bed infiltration also has an important effect on flood propagation as the flood waves travel downstream to the catchment outlet. Hence, wadi bed infiltration may be the predominant process underlying groundwater recharge. Quantification of the infiltration loss is thus important. Sorman and Abdulrazzak (1993) estimate that on average, 75% of bed infiltration reaches the water table, according to an experimental reach in Wadi Tabalah, located in southwestern Saudi Arabia. In the present work, depths of infiltration losses are estimated by subtracting the direct runoff from the precipitation of each subcatchment. The infiltrated volume is then quantified, taking into account the aerial extent of each subcatchment.

Locating sites with possibly high flash flood and groundwater potentials

In order to demarcate sites with the highest potential for flood risk on road networks, as well as those that may be used for artificially recharging groundwater, a DEM-based relative stream power (RSP) index and WI were derived. These indices were assumed to affect soil characteristics, distribution and abundance of soil water, susceptibility of landscapes to erosion by water, and the distribution and abundance of flora and fauna (Moore et al. 1991; Wilson and Gallant 2000). Moore et al. (1993) state that such terrain attributes significantly correlate with the measured soil properties.

RSP is the time rate of energy expenditure and has been used extensively in studies of erosion, sediment transport, and geomorphology as a measure of the potential erosive power of the overland flows (Moore et al. 1991; Moore et al. 1993). It is usually computed as:

$$\mathrm{RSP} = \rho g q \tan\beta \tag{6}$$

where ρg is the unit weight of water, q is the discharge per unit width, and β is the slope gradient (in degrees). Since ρg is constant and the discharge (q) is often assumed to be proportional to specific catchment area (A_s), the index ($A_s \tan\beta$) is, therefore, a measure of the stream power. RSP predicts net erosion in areas of profile convexity and tangential concavity (flow acceleration and convergence zones) and net deposition in areas of profile concavity (zones of decreasing flow velocity). As the gradient of specific catchment areas increases, the amount of water contributed by the upslope areas and the velocity of water flow increase, hence stream power index and erosion risk increase.

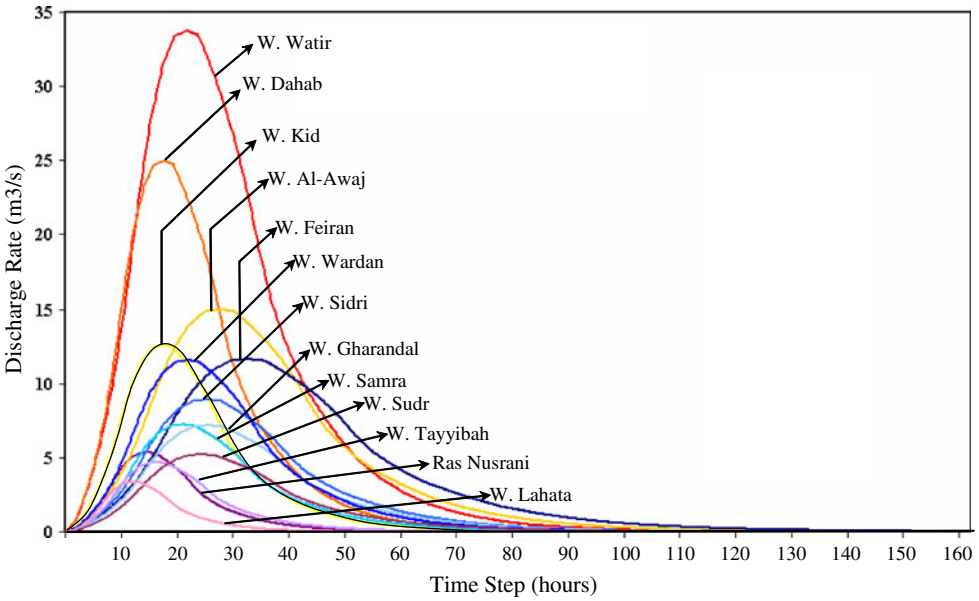

Fig. 7 Unit hydrographs of the studied catchments

The WI is also based on the idea that the area of the local slope and upslope affect soil moisture conditions. Wetness index is computed as:

$$\mathrm{WI} = \ln\left(\frac{A_s}{\tan\beta}\right) \tag{7}$$

The higher the value of WI, the higher the possibility of a land unit remaining wet after a flood. This is one possible measure that can be recommended for use in order to recharge groundwater.

Pixels located within a 200-m buffer zone from the road networks that have the maximum logarithm of RSP (6–8) values are proposed to have the highest potential for flood risks. Also, sites with the highest (26.5–29.5 WI) values located within a 300-m buffer zone from the faults are recommended sites for recharging groundwater aquifers. The logarithm of the RSP is further classified into two classes, from 0–4 and 4–8, and their areal extents are estimated for each catchment. The area coverage of the two classes have been correlated with the UH peak discharge, hydrograph peak discharge, and runoff volume.

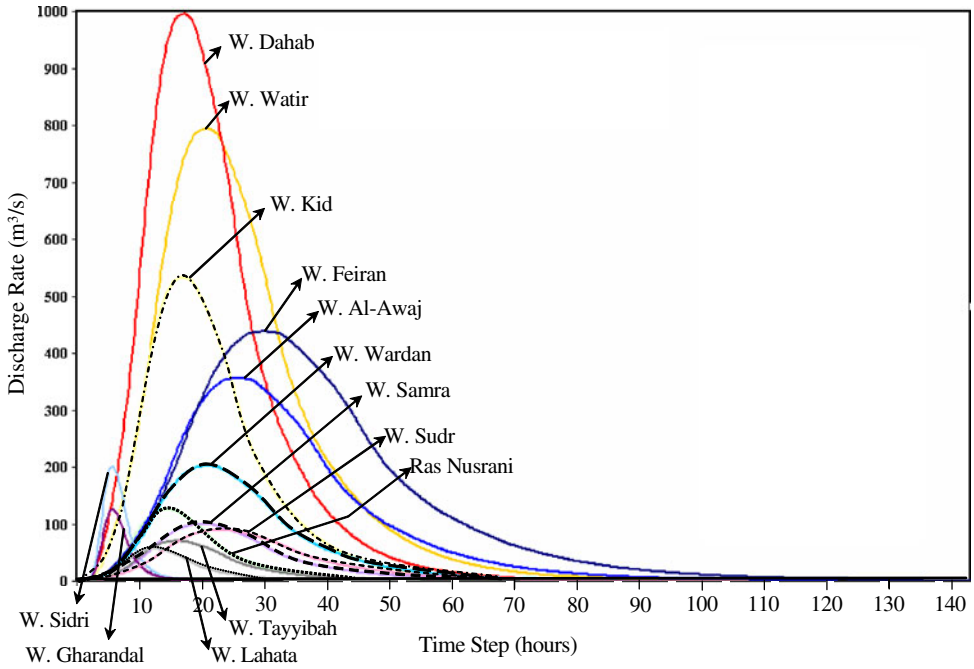

Fig. 8 Hydrographs of the studied catchments

Results

The predicted unit hydrographs and catchments hydrographs are shown on Figs. 7 and 8, respectively. The lag time and predicted peak discharge rates, along with the volumes of rainfall, runoff, and abstraction losses are summarized in Table 4. The shape of the UH and hydrographs had relatively symmetrical rising and falling limbs. The UH and hydrographs showed steep rising and falling limbs for the W. Watir and W. Dahab catchments, and a slight increase for the rest of the catchments. The predicted UH and hydrograph peak discharges of the W. Watir were 33.75 ($m^3/s/km^2/mm$) and 793 m^3/s, respectively. W. Dahab catchment showed 24.97 ($m^3/s/km^2/mm$) and 993 m^3/s for the UH and hydrograph peak discharge rates, respectively. For the remaining catchments, the UH varied from 3.36 to 15 ($m^3/s/km^2/mm$), and the peak discharges of the hydrographs ranged from 56 to 532 m^3/s. In terms of catchments peak discharge rates, the

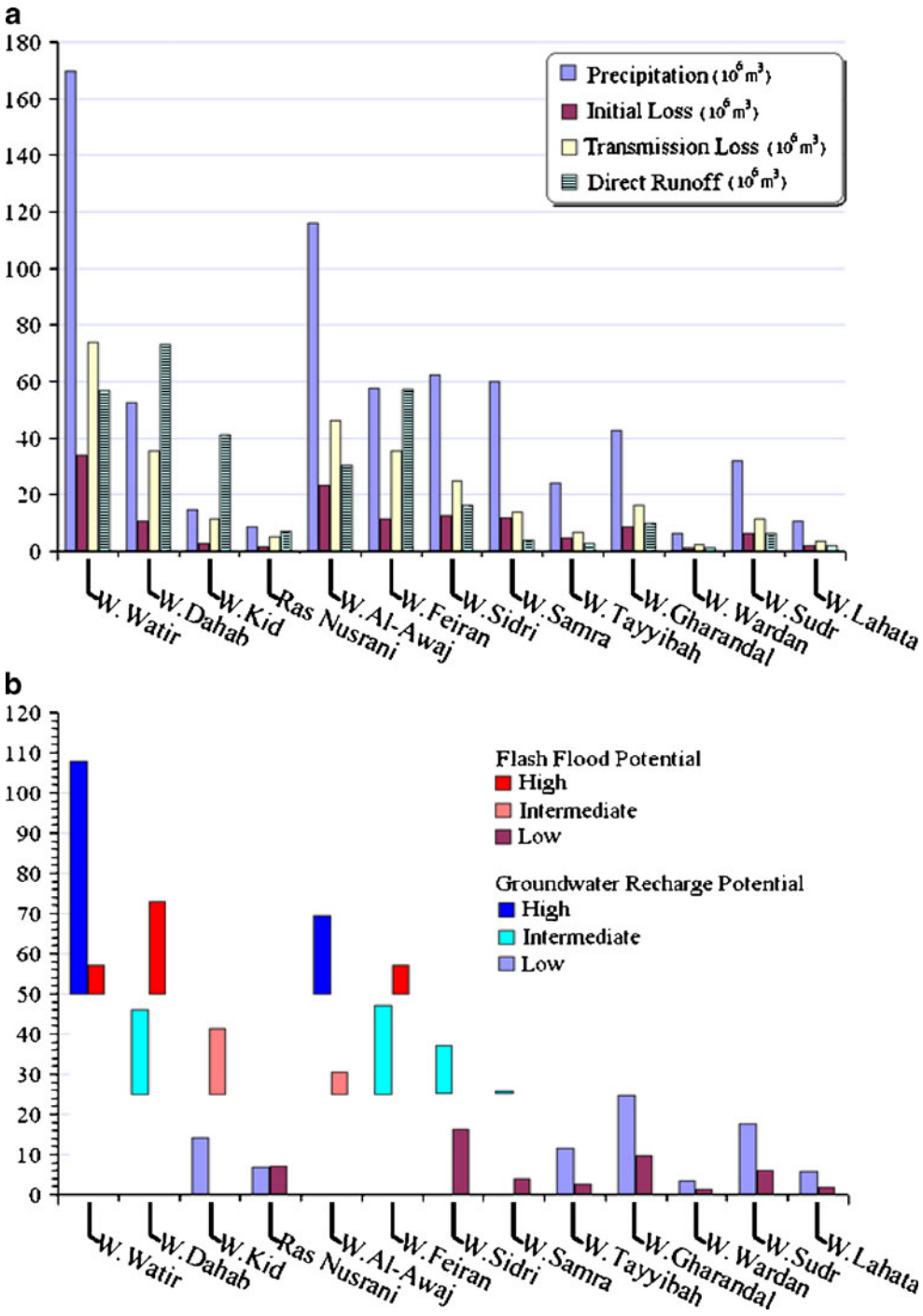

Fig. 9 Diagram showing the runoff-infiltration characteristics of the studied catchments; **a** runoff-infiltration volumes and **b** classes of flash flood and groundwater recharge potential

W. Dahab catchment had the highest rate followed by the W. Watir, W. Kid, W. Feiran, and W. Al-Awaj catchments, with rates in total ranging from 993 to 356 m^3/s. The remaining catchments showed relatively low rates in a range between 201 (W. Wardan catchment) and 56 (W. Lahata catchment) m^3/s. Transformation of the UH to the catchments hydrograph showed linearity for the studied catchments, with the exceptions of the W. Dahab and W. Fieran catchments. This comes from the higher contribution of the topography (divide average relief) and hence the precipitation.

Catchments were then classified according to their direct runoff and infiltration volumes. Infiltration volumes were estimated by summing the initial and transmission losses. Three main classes were assigned to figure out the potentiality: high ($>50\times10^6$ m^3), intermediate (25×10^6 m^3 -50×10^6 m^3), and low (1.28×10^6 m^3 -25×10^6 m^3). The runoff-infiltration volumes as well as the classes of the flash flood and groundwater potential are shown on Fig. 9. Among the catchments predicted to have high flash flood potential, the catchment of W. Dahab showed the highest rank followed by the W. Fieran and W. Watir catchments. W. Kid and W. Al-Awaj had an intermediate potential. The catchments of W. Sidri, W. Gharandal, Ras Nusrani, W. Sudr, W. Samra, W. Tayyibah, W. Lahata, and W. Wardan showed low potential. Among the catchments that had high groundwater recharge potential, W. Watir had the highest potential followed by W. Al-Awaj. The catchments of W. Feiran, W. Dahab, W. Sidri, and W. Samra had intermediate groundwater potential. W. Gharandal, W. Sudr, W. Kid, W. Tayyibah, Ras Nusrani, W. Lahata, and W. Wardan fell within the low potential class. The catchments have been listed according to their estimated runoff and infiltration volumes in a descending order from highest to lowest within each class. Górski and Ghodeif (2000) stated that the recharge rate (32,000 m^3/day) of the Quaternary aquifer underlying the Qaa Plain where W. Al-Awaj flows exceeds the discharge (26,000 m^3/day) and the static water level showed no distinct change since 1972. Thus, W. Watir could be promising for groundwater exploration as it has even higher potential than W. Al-Awaj.

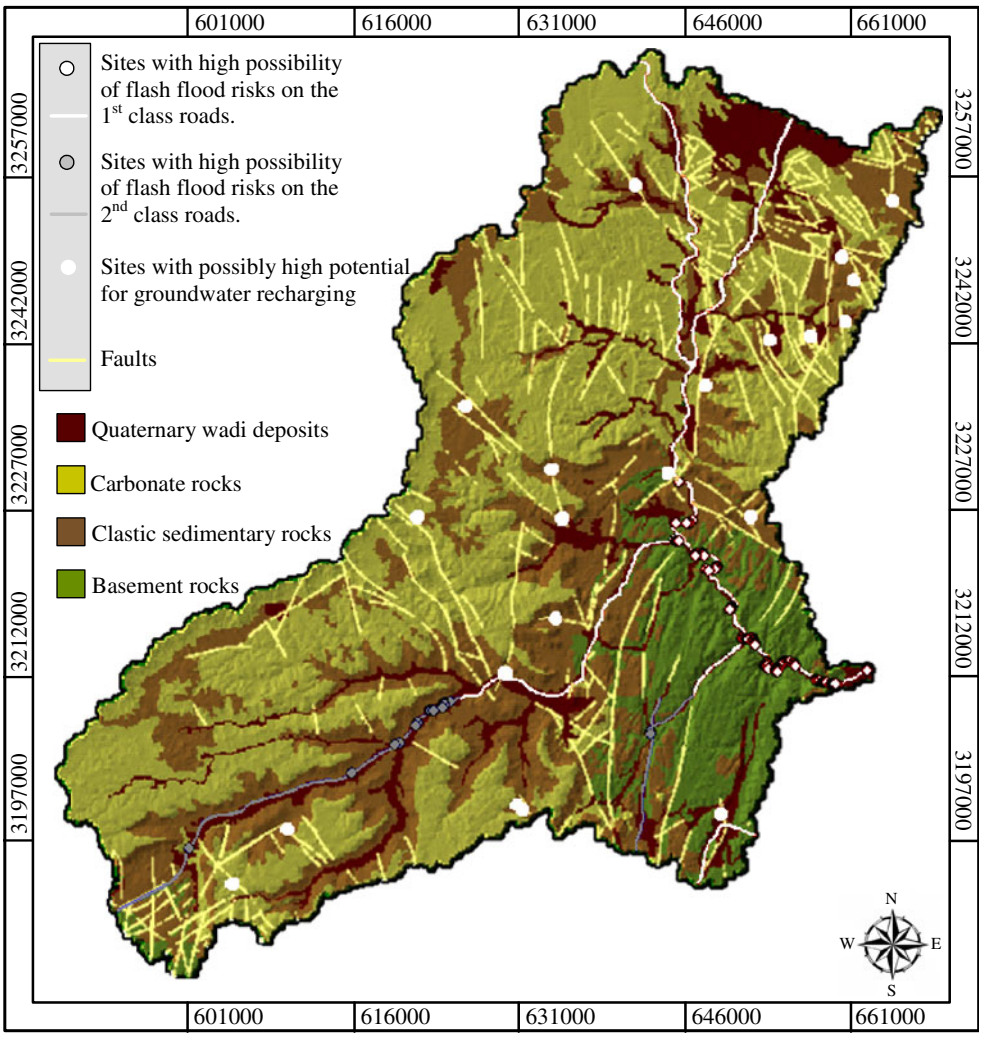

Fig. 10 Located sites for possible high flash flood risks and groundwater recharging in Wadi Watir displayed over the regional geology draped over DEM

The present rainfall–runoff model showed a rainfall volume sum of 725.5×10^6 m^3. The distribution of the total rainfall over the three components was: runoff volume of 307.8×10^6 m^3 (43.4%), initial loss of 131.5×10^6 m^3 (18.1%), and 286×10^6 m^3 (39.4%) transmission loss. The estimated recharge volume proposed to recharge the shallow groundwater aquifers underlying the studied catchments counted for about 57.5% of the total rainfall that corresponds well with that of the JICA (1999). According to JICA (1999), an estimated recharge resulting from individual large storm expected every 60 years (76 mm) over the mountainous St. Catherine area was 135.4×10^6 m^3(50% of the total precipitation). Infiltration losses are found to be more effective than runoff flows in catchments with dominant wadi bed coverage having relatively low CN. While for the catchments with high values of the CN with hard rock cover is dominating, the runoff flow is larger than the infiltration abstraction.

Located sites for possible high flash flood risks and groundwater recharging are shown on Fig. 10 for Wadi Watir and on Fig. 11 for the whole studied catchments. Field visits to most of the sites confirmed the validity of the adopted methodology. There were many sections of the road network that were washed out during previous flood occurrences. Also, there were abandoned and remnants of the hydraulic structures built for flood-spreading found on some of the subcatchment piedmont areas and foothills. About 50% of the sites demarcated to likely have high potential for groundwater recharging there found wells dug for domestic use by the local Beduin in particular in W. Feiran, W. Sidr, St. Catherine area, and Sudr and Qaa Plains where shallow Quaternary aquifer underlie the terrain.

Model evaluation

Evaluation of the modeling results relies on the availability of proper reference data. There is a worldwide lack of published reports addressing the rainfall and water balance

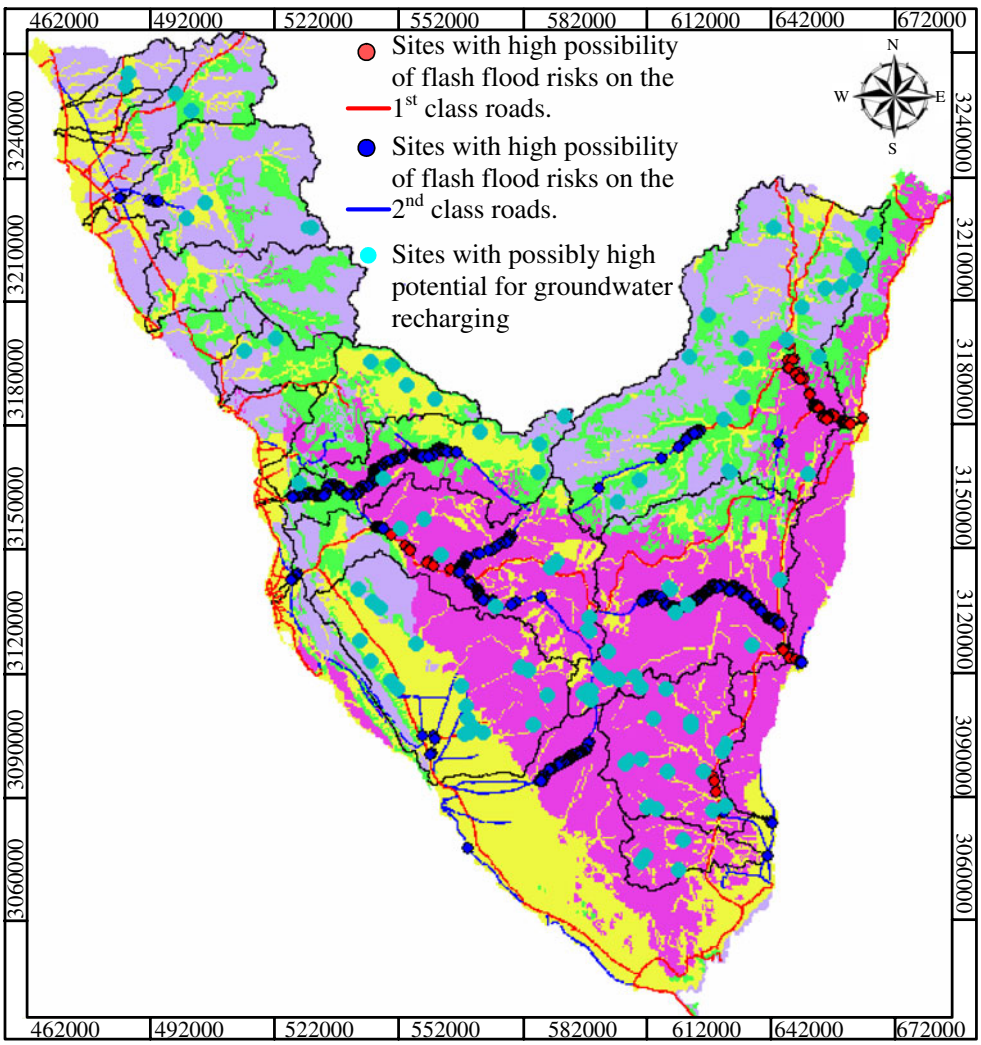

Fig. 11 Located sites for possible high potential for flash flood risks on the road networks and groundwater recharging in the studied catchments

Table 3 Rock-soil classes of W. Watir catchment

Geologic age	Code	Description
Holocene	Qw	Wadi deposits
Pleistocene	Qfg	Fanglomerates
Pleistocene	Qh	Alluvial Hamadah deposits
Miocene	Tmqb	Fossiliferous limestone
Middle Eocene	Temk	Limestone with banks of *Nummulites*
Late Eocene	Teleg	Chalky limestone with flint/chert bands and nodules
Paleocene	Tpes	Shales with soft marl
Cretaceous (Maast.-Camp.)	Ksd	Limestone with marl and clay beds in the lower part
Cretaceous (Campanian)	Kdu	Alternates of chert-capped clastics and carbonates
Cretaceous (Turonian)	Kwt	Limestone with shale intercalations
Cretaceous	Kv	Basaltic dykes
Cretaceous (Cenomanian)	Kjll	Marl capped with limestone
Cretaceous (Albian–Aptian)	Kml	Sandstone with kaolinitic pockets
Mesozoic (Jurassic)	Jrq	Sandstone
Paleozoic (Cambrian)	€nq	Quartzitic sand and sandstone
	€ar	Ferruginous sandstone with sandy clay bands
Late Proterozoic	ckg	Granites
	gmg	Monzonites
	gd	Diorite and granodiorite
	md	Metadiorite with mafic xenoliths

estimates; in particular, for ungauged catchments of the arid regions. Luckily, Milewski et al. (2009) estimated the average annual (1998–2007) rainfall, initial abstraction, runoff, and the transmission losses for three out of the studied catchments: W. Watir, W. Dahab, and W. Al-Awaj catchments. These estimates are based on calibration of the 3-hourly precipitation from the Tropical Rainfall Measuring Mission data for W. Girafi catchment in Sinai using stream flow data collected at the outlet of the catchment in Israel. Rainfall estimates from the present study for the catchments of W. Watir, W. Dahab, and W. Al-Awaj showed values of 164.9×10^6 m^3, 118.8×10^6 m^3, and 100×10^6 m^3, respectively. These estimates agree well with those reported in Milewski et al. (2009), where these catchments showed average annual (1998–2007) of 192.7×10^6 m^3, 110.6×10^6 m^3, and 74.2×10^6 m^3, respectively.

Results from the present study indicated an average runoff of 42.15% and average transmission loss of 40.27%

Table 4 The curve number, UH, hydrograph, and rainfall–runoff characteristics of the studied catchments

Catchment	CN	T_{lag} (h)	UH Peak Discharge (m^3/s)	Catchment peak discharge (m^3/s)	P (mm)	Q (mm)	I_a (mm)	Rainfall (10^6m^3)	Runoff (10^6m^3)	Initial loss (10^6m^3)	Transmission loss (10^6m^3)
W. Watir	83.8	21.22	33.75	793	47.68	16.48	9.82	164.93	57.01	33.96	73.94
W. Dahab	90.9	17.14	24.97	993	57.45	35.24	5.08	118.86	72.92	10.52	35.41
W. Kid	94.8	17.07	12.56	532	53.44	39.72	2.78	55.47	41.23	2.89	11.34
Ras Nusrani	91.3	14.11	5.35	125	38.24	19.36	4.84	13.96	7.06	1.76	5.12
W. Al-Awaj	81.0	26.96	15	356	51.3	15.67	11.91	100.04	30.56	23.23	46.23
W. Feiran	88.7	31.78	11.62	437	58.41	32.00	6.47	104.15	57.05	11.54	35.54
W. Sidri	81.2	24.68	8.9	199	50.28	15.24	11.76	53.40	16.18	12.49	24.71
W. Samra	75.1	20.45	7.21	100	41.52	5.59	16.84	29.65	3.99	12.02	13.62
W. Tayyibah	79.0	15.85	4.67	70	40.07	7.50	13.50	14.35	2.68	4.83	6.82
W. Gharandal	83.7	24.93	7.16	125	40.07	11.43	9.89	34.54	9.85	8.52	16.15
W. Wardan	83.1	21.32	11.55	201	39.99	10.81	10.33	4.76	1.28	1.23	2.24
W. Sudr	82.6	23.71	5.2	89	39.95	10.33	10.70	23.77	6.15	6.37	11.25
W. Lahata	81.9	11.71	3.36	56	40.02	9.76	11.22	7.60	1.85	2.13	3.61

for the above-mentioned catchments. These results correspond well with the reported and inferred average transmission losses in several similar arid catchments that were found to exceed 40% from the total rainfall. Milewski et al. (2009) reported an average annual runoff of 6.1% and average annual recharge through transmission losses of 23.9% for these catchments. WRRI/JICA (1999) showed an average of 14% runoff and 54% transmission losses from the total rainfall for the Sinai Peninsula. Morin et al. (2009) indicated an average annual recharge (1960-2005) of 42.67% from the ephemeral arid Kuiseb River segments in Namibia. In this river, inferred transmission losses from simulated discharges averaged 56.72% (Table 3 in Lange 2005). Miller et al. (2005) reported approximately 40% transmission losses throughout an experimental channel in Nevada desert. Costelloe et al (2003) reported transmission losses ranging between 70% and 98%. Telvari et al. (1998) stated that approximately two thirds of overland flow is transmitted downstream once the alluvial storage is satisfied. From this review, it seems that the modeling results of Milewski et al. (2009), despite calibrated, is underestimated. Underestimation of results can be proofed from the comparison of the calibrated model variables for the wadi Asyuti and Hammamat catchments located in the Eastern Desert of Egypt shown on Table 1 in Gheith and Sultan (2002) and on Table 4 in Milewski et al. (2009). Generalization of calibrated parameters can never suite all catchments due to the

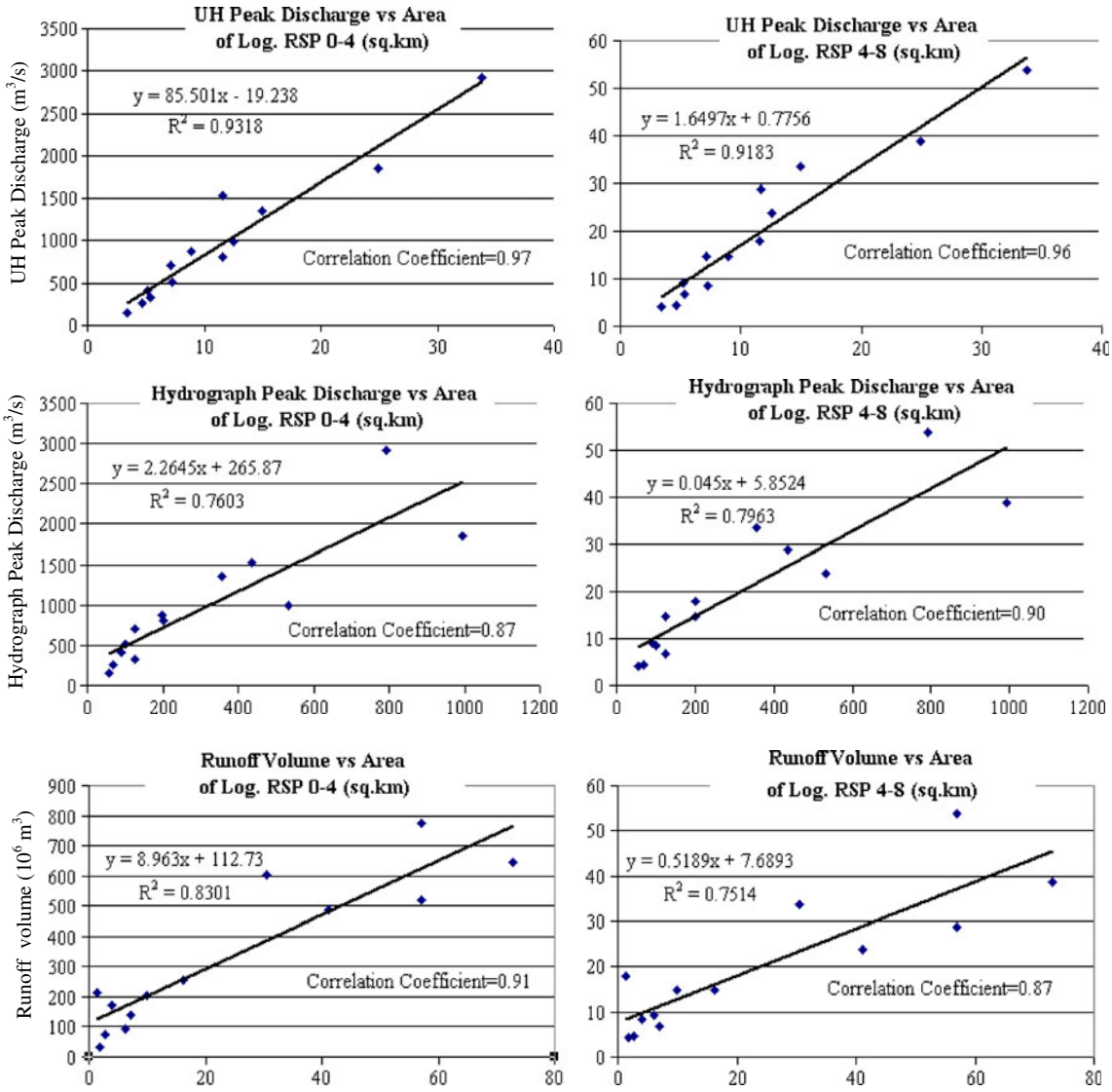

Fig. 12 Diagrams showing correlation coefficient and R^2 between the coverage of the log RSP (km^2) from 0–4 (*left*) and 4–8 (*right*), and the runoff characteristics including the UH peak discharge (m^3/s), hydrograph peak discharge (m^3/s), and the runoff volume (10^6 m^3) of the studied catchments

variability of the surficial geomorphic characteristics and infiltration capacities.

In order to overcome this problem, an alternative approach that can relate catchment responses to its characteristics is advisable in minimizing modeling parameter uncertainty (Wheater 2005). For this, various catchment characteristics were correlated with the model parameters. The areal extent of the RSP achieved the best correlation. Figure 12 clarifies the correlation between the areal coverage of the two classes derived from the RSP with the UH peak discharge (correlation coefficient >0.96 and R^2>0.91), hydrograph peak discharge (correlation coefficient >0.87 and R^2>0.76), and the runoff volume (correlation coefficient >0.87 and R^2>0.75). This correlation establishes the validity of this single parameter to predict the runoff potential of the catchments. This could be a promising alternative to validate the runoff models when reference discharge data are unavailable.

Conclusions

The methodology adopted and the developed runoff models, despite being simply limited by the lack of proper hydrometeorological data, represent a crucial premise for better understanding the hydrological phenomena in the wadi systems of the arid desert environments where such studies are rare. The predicted hydrographs, the runoff-infiltration volume estimates, and the sites demarcated to possibly have high potential for the flash flood, and the groundwater recharge could improve the solutions for the flood risk mitigation and the availability of water from the wadi systems. Despite the lack of discharge data, the secondary topographic indices coupled with the field observations were useful in validating the resulted models. Construction of runoff controlling systems in the proposed areas could lessen the flood vulnerability and save and make use of a considerable amount of water to meet part of the ever growing water needs in these harsh environments. A master planning of the entire catchments not only with respect to the flood risk and water use, but as much so for tourism, wadi habitats, and more is direly needed. New and advanced methodologies and data acquisition techniques are essential to predict the hydrologic and other relevant environmental data about the ungauged catchments. So, there is an urgent need for research in this direction to facilitate appropriate policy measures.

Acknowledgments I am grateful to the anonymous reviewers for their constructive comments on the article. I would like to acknowledge the help of the jeep driver, Mr. Mahmoud Temraz, during the field campaigns. I am also thankful to the staff at the Governorate of Southern Sinai and the Scientific Research Academy in Cairo for their help in securing flash flood reports available for the study area.

References

Ajami NK, Gupta H, Wagener T, Sorooshian S (2004) Calibration of a semi-distributed hydrologic model for streamflow estimation along a river system. J Hydrol 298:112–135

Beven KJ (1996) Response to comments on 'A discussion of distributed hydrological modelling' by J.C. Refsgaard et al. 1996. In: Abbott MB, Refsgaard JC (eds) Distributed hydrological modelling. Kluwer Academic, Dordrecht, pp 289–295

Chow VT, Maidment DR, Mays LW (1988) Applied hydrology. McGraw-Hill, New York, p 572

Congalton RG (1991) A review of assessing the accuracy of classifications of remotely sensed data. Remote Sens Environ 37(1):35–46

Costelloe JF, Grayson RB, Argent RM, McMahon TA (2003) Modelling the flow regime of an arid zone floodplain river, Diamantina River, Australia. Environ Model Softw 18(8):693–703

Cunge JA (1969) On the subject of a flood propagation computation method (Muskingum method). J Hydraul Res 7(2):205–230

Dames and Moore (1985) Sinai development Report, phase 1, final report **5**, water supplies and costs. Submitted to the Advisory Committee for Reconstruction Ministry of Development, Cairo

Duan Q, Gupta HV, Sorooshian S, Rousseau AN, Turcotte R (2003) Calibration of watershed models. Water Science and Application. American Geophysical Union, Washington, p 345

Egyptian Meteorological Authority (1996) Climatic Atlas of Egypt. Ministry of Transport and Communications, Cairo

El-Hames AS, Richards KS (1994) Progress in arid-lands rainfall-runoff modeling. Prog Phys Geogr 18(3):343–365

Farr TG, Kobrick M (2000) Shuttle radar topography mission produces a wealth of data, Eos Transactions. American Geophysical Union 81(48):583–585

Foody GM, Ghoneim EM, Arnell NW (2004) Predicting locations sensitive to flash flooding in an arid environment. J Hydrol 292 (1–4):48–58

Freeman TG (1991) Calculating catchment area with divergent flow based on a regular grid. Comput Geosci 17(3):413–422

Geological Map of Sinai, Arab Republic of Egypt (1994) (Sheet No. 1, 2 and 3), Scale 1:250 000.

Gheith H, Sultan M (2002) Construction of a hydrology model for estimating wadi runoff and groundwater recharge in the Eastern Desert, Egypt. J Hydrol 263:36–55

Górski J, Ghodeif K (2000) Salinization of Shallow Water Aquifer in El-Qaa Coastal Plain, Sinai, Egypt. In: Sadurski, A. (ed.) Proceedings of SWIM 16, Międzyzdroje-Wolin Island, Poland, 12–15 June, Nicholas Copernicus University vol. 80, pp 63–72

Graf WL (1988) Definition of flood plains along arid-region rivers. In: Baker VR, Kochel RC, Patton PC (eds) Flood geomorphology. Wiley, New York, pp 231–242

GRASS Development Team (2006) Geographic Resources Analysis Support System (GRASS) Software. ITC-irst, Trento, Italy. http://grass.itc.it.

Gray DM (1961) Synthetic unit hydrographs for small watersheds. J Hydraul Div ASCE 87(4):33–54

Headman FR (1970) Mean annual runoff as related to channel geometry of selected streams on California. USGS-WSP, 1999-E, p 17

Hickok RB, Keppel RV, Rafferty BR (1959) Hydrograph synthesis for small arid land watersheds. Agric Eng 40(10):608–611

Jenson SK, Domingue JO (1988) Extracting topographic structure from digital elevation data for geographic information system analysis. Photogramm Eng Remote Sensing 54(11):1593–1600

JICA - Japan International Cooperation Agency, 1999. South Sinai Groundwater Resources Study Report, Pacific Consultants International and Sanyu Consultants Inc., Tokyo

Klemeš V (1986) Operational testing of hydrologic simulation models. J Hydrol Sci 31:13–23

Kokkonen TS, Jakeman AJ, Young PC, Koivusalo HJ (2003) Predicting daily flows in ungauged catchments: model regionalization from catchment descriptors at the Coweeta Hydrologic Laboratory, North Carolina. Hydrol Process 17:2219–2238

Lane LJ (1972) A proposed model for flood routing in abstracting ephemeral channels. Hydrol Water Resour Ariz Southwest 2 (2):439–453

Lange J (2005) Dynamics of transmission losses in a large arid stream channel. J Hydrol 306(1–4):112–126

Lindsay JB, Creed IF (2005) Removal of artifact depressions from digital elevation models: towards a minimum impact approach. Hydrol Process 19(6):3113–3126

Littlewood IG (2002) Improved unit hydrograph characterization of the daily flow regime (including low flows) for the River Teifi, Wales: towards better rainfall–streamflow models for regionalization. Hydrol Earth Syst Sci 6(5):899–911

Masoud A (2003) An integrated remote sensing and GIS approach for flash flood potential, mitigation, and floodwater resource management: development and application on Safaga area, Egypt. Ph. D. Dissertation, Osaka City University, Japan, p 288

Michaud J, Sorooshian S (1994) Comparison of simple versus complex distributed runoff models on a midsized semiarid watershed. Water Resour Res 30(3):593–605

Milewski A, Sultan M, Eugene Y, Abdeldayem A, Abdel Gelil K (2009) A remote sensing solution for estimating runoff and recharge in arid environments. J Hydrol 373:1–14

Miller JJ, Mizell SA, French RH, Meadows DG, Young MH (2005) Channel Transmission Loss Studies During Ephemeral Flow Events: ER-5-3 Channel and Cambric Ditch, Nevada Test Site, Nye County, Nevada, Technical Report, DOE/NV/13609 - 42, Desert Research Institute, Nevada System of Higher Education, p 66

Moore ID, Gessler PE, Nielsen GA, Peterson GA (1993) Soil attribute prediction using terrain analysis. Soil Sci Soc Am J 57(2):443–452

Moore ID, Grayson RB, Ladson AR (1991) Digital terrain modeling: a review of hydrological, geomorphological and biological applications. Hydrol Process 5(1):3–30

Morin E, Grodek T, Dahan O, Benito G, Kulls C, Jacoby Y, Van Langenhove G, Seely M, Enzel Y (2009) Flood routing and alluvial aquifer recharge along the ephemeral arid Kuiseb River, Namibia. J Hydrol 368(1-4):262–275

Moussa R, Chahinian N, Bocquillon C (2007) Distributed hydrological modeling of a Mediterranean mountainous catchment – model construction and multi-site validation. J Hydrol 337:35–51

Murphey JB, Wallace DE, Lane LJ (1977) Geomorphic parameters predict hydrograph characteristics in the southwest. Water Resour Bull 13(1):25–38

Quinn P, Beven K, Chevallier P, Planchon O (1991) The prediction of hillslope flow paths for distributed hydrological modeling using digital terrain models. Hydrol Process 5:59–80

Quinn P, Beven K, Lamb R (1995) The ln(a/tan beta) index: how to calculate it and how to use it within the TOPMODEL framework. Hydrol Process 9(2):161–182

Refsgaard JC (1997) Parametrisation, calibration, and validation of distributed hydrological models. J Hydrol 198:69–97

Said R (1962) The geology of Egypt. Elsevier, New York 377

Soil Conservation Service (SCS) (1972) Estimation of direct runoff from storm rainfall, National Engineering Handbook. Section 4-Hydrology, 10.1–10.24

Sharma KD, Murthy JSR (1994) Estimating transmission losses in an arid region. J Arid Environ 26(3):209–219

Sharma KD, Murthy JSR (1995) Hydrologic routing of flow in arid ephemeral channels. J Hydraul Eng ASCE 121(6):466–471

Sefton CEM, Howarth SM (1998) Relationships between dynamic response characteristics and physical descriptors of catchments in England and Wales. J Hydrol 211:1–16

Sorman AU, Abdulrazzak MJ (1993) Infiltration-recharge through wadi beds in arid regions. Hydrol Sci J 38(3):173–186

Schlesinger S, Crosbie RE, Gagné RE, Innis GS, Lalwani CS, Loch J, Sylvester J, Wright RD, Kheir N, Bartos D (1979) Terminology for model credibility. SCS Technical Committee on Model Credibility. Simulation 32(3):103–104

Tarboton DG (1997) A new method for the determination of flow directions and contributing areas in grid digital elevation models. Water Resour Res 33(2):309–319

Telvari A, Cordery I, Pilgrim DH (1998) Relations between transmission losses and bed alluvium in an Australian arid zone stream. In: Wheater H, Kirby C (eds) Hydrology in a Changing Environment, vol. II. Wiley, pp 361–36

Valdes JB, Fiallo Y, Rodriguez-Iturbe I (1979) A rainfall–runoff analysis of the geomorphologic IUH. Water Resour Res 15 (6):1421–1434

Wagener T, Wheater H, Gupta HV (2004) Rainfall–runoff modeling in gauged and ungauged catchments. Imperial College Press, London 306

Walters MO (1990) Transmission losses in arid region. J Hydraul Eng 116(1):129–138

Wheater HS (2005) Modeling Hydrological Processes in Arid and Semi Arid Areas,. Proceedings of the GWADI International Modeling Workshop, Roorkee, India, p 39 http://www.geadi.org/shortcourses

Wilson JP, Gallant JC (2000) Secondary topographic attributes. In: Wilson JP, Gallant JC (eds) Terrain analysis: principles and applications. Wiley, New York, pp 87–132

Yair A, Lavee H (1985) Runoff generation in arid and semiarid zones. In: Anderson MG, Burt TP (eds) Hydrological forecasting. Wiley, New York, pp 183–220 Chap.8

Yen BC, Lee KT (1997) Unit hydrograph derivation for ungauged catchments by stream-order laws. J Hydraul Eng 2(1):1–9